Measurement of the Helicity Fractions of W Bosons from Top Quark Decays using Fully Reconstructed $t\bar{t}$ Events with CDF II

A. Abulencia,[24] J. Adelman,[13] T. Affolder,[10] T. Akimoto,[56] M.G. Albrow,[17] D. Ambrose,[17] S. Amerio,[44]
D. Amidei,[35] A. Anastassov,[53] K. Anikeev,[17] A. Annovi,[19] J. Antos,[14] M. Aoki,[56] G. Apollinari,[17] J.-F. Arguin,[34]
T. Arisawa,[58] A. Artikov,[15] W. Ashmanskas,[17] A. Attal,[8] F. Azfar,[43] P. Azzi-Bacchetta,[44] P. Azzurri,[47]
N. Bacchetta,[44] W. Badgett,[17] A. Barbaro-Galtieri,[29] V.E. Barnes,[49] B.A. Barnett,[25] S. Baroiant,[7] V. Bartsch,[31]
G. Bauer,[33] F. Bedeschi,[47] S. Behari,[25] S. Belforte,[55] G. Bellettini,[47] J. Bellinger,[60] A. Belloni,[33] D. Benjamin,[16]
A. Beretvas,[17] J. Beringer,[29] T. Berry,[30] A. Bhatti,[51] M. Binkley,[17] D. Bisello,[44] R.E. Blair,[2] C. Blocker,[6]
B. Blumenfeld,[25] A. Bocci,[16] A. Bodek,[50] V. Boisvert,[50] G. Bolla,[49] A. Bolshov,[33] D. Bortoletto,[49] J. Boudreau,[48]
A. Boveia,[10] B. Brau,[10] L. Brigliadori,[5] C. Bromberg,[36] E. Brubaker,[13] J. Budagov,[15] H.S. Budd,[50] S. Budd,[24]
S. Budroni,[47] K. Burkett,[17] G. Busetto,[44] P. Bussey,[21] K. L. Byrum,[2] S. Cabrera[o],[16] M. Campanelli,[20]
M. Campbell,[35] F. Canelli,[17] A. Canepa,[49] S. Carillo[i],[18] D. Carlsmith,[60] R. Carosi,[47] M. Casarsa,[55] A. Castro,[5]
P. Catastini,[47] D. Cauz,[55] M. Cavalli-Sforza,[3] A. Cerri,[29] L. Cerrito[m],[43] S.H. Chang,[28] Y.C. Chen,[1]
M. Chertok,[7] G. Chiarelli,[47] G. Chlachidze,[15] F. Chlebana,[17] I. Cho,[28] K. Cho,[28] D. Chokheli,[15] J.P. Chou,[22]
G. Choudalakis,[33] S.H. Chuang,[60] K. Chung,[12] W.H. Chung,[60] Y.S. Chung,[50] T. Chwalek,[26] M. Ciljak,[47]
C.I. Ciobanu,[24] M.A. Ciocci,[47] A. Clark,[20] D. Clark,[6] M. Coca,[16] G. Compostella,[44] M.E. Convery,[51] J. Conway,[7]
B. Cooper,[36] K. Copic,[35] M. Cordelli,[19] G. Cortiana,[44] F. Crescioli,[47] C. Cuenca Almenar,[7] J. Cuevas[l],[11]
R. Culbertson,[17] J.C. Cully,[35] D. Cyr,[60] S. DaRonco,[44] M. Datta,[17] S. D'Auria,[21] T. Davies,[21] M. D'Onofrio,[3]
D. Dagenhart,[6] P. de Barbaro,[50] S. De Cecco,[52] A. Deisher,[29] G. De Lentdecker[c],[50] M. Dell'Orso,[47] F. Delli Paoli,[44]
L. Demortier,[51] J. Deng,[16] M. Deninno,[5] D. De Pedis,[52] P.F. Derwent,[17] G.P. Di Giovanni,[45] C. Dionisi,[52]
B. Di Ruzza,[55] J.R. Dittmann,[4] P. DiTuro,[53] C. Dörr,[26] S. Donati,[47] M. Donega,[20] P. Dong,[8] J. Donini,[44]
T. Dorigo,[44] S. Dube,[53] J. Efron,[40] R. Erbacher,[7] M. Erdmann,[26] D. Errede,[24] S. Errede,[24] R. Eusebi,[17]
H.C. Fang,[29] S. Farrington,[30] I. Fedorko,[47] W.T. Fedorko,[13] R.G. Feild,[61] M. Feindt,[26] J.P. Fernandez,[32] R. Field,[18]
G. Flanagan,[49] A. Foland,[22] S. Forrester,[7] G.W. Foster,[17] M. Franklin,[22] J.C. Freeman,[29] I. Furic,[13] M. Gallinaro,[51]
J. Galyardt,[12] J.E. Garcia,[47] F. Garberson,[10] A.F. Garfinkel,[49] C. Gay,[61] H. Gerberich,[24] D. Gerdes,[35] S. Giagu,[52]
P. Giannetti,[47] A. Gibson,[29] K. Gibson,[48] J.L. Gimmell,[50] C. Ginsburg,[17] N. Giokaris[a],[15] M. Giordani,[55]
P. Giromini,[19] M. Giunta,[47] G. Giurgiu,[12] V. Glagolev,[15] D. Glenzinski,[17] M. Gold,[38] N. Goldschmidt,[18]
J. Goldstein[b],[43] A. Golossanov,[17] G. Gomez,[11] G. Gomez-Ceballos,[11] M. Goncharov,[54] O. González,[32] I. Gorelov,[38]
A.T. Goshaw,[16] K. Goulianos,[51] A. Gresele,[44] M. Griffiths,[30] S. Grinstein,[22] C. Grosso-Pilcher,[13] R.C. Group,[18]
U. Grundler,[24] J. Guimaraes da Costa,[22] Z. Gunay-Unalan,[36] C. Haber,[29] K. Hahn,[33] S.R. Hahn,[17]
E. Halkiadakis,[53] A. Hamilton,[34] B.-Y. Han,[50] J.Y. Han,[50] R. Handler,[60] F. Happacher,[19] K. Hara,[56] M. Hare,[57]
S. Harper,[43] R.F. Harr,[59] R.M. Harris,[17] M. Hartz,[48] K. Hatakeyama,[51] J. Hauser,[8] A. Heijboer,[46] B. Heinemann,[30]
J. Heinrich,[46] C. Henderson,[33] M. Herndon,[60] J. Heuser,[26] D. Hidas,[16] C.S. Hill[b],[10] D. Hirschbuehl,[26] A. Hocker,[17]
A. Holloway,[22] S. Hou,[1] M. Houlden,[30] S.-C. Hsu,[9] B.T. Huffman,[43] R.E. Hughes,[40] U. Husemann,[61]
J. Huston,[36] J. Incandela,[10] G. Introzzi,[47] M. Iori,[52] Y. Ishizawa,[56] A. Ivanov,[7] B. Iyutin,[33] E. James,[17]
D. Jang,[53] B. Jayatilaka,[35] D. Jeans,[52] H. Jensen,[17] E.J. Jeon,[28] S. Jindariani,[18] M. Jones,[49] K.K. Joo,[28]
S.Y. Jun,[12] J.E. Jung,[28] T.R. Junk,[24] T. Kamon,[54] P.E. Karchin,[59] Y. Kato,[42] Y. Kemp,[26] R. Kephart,[17]
U. Kerzel,[26] V. Khotilovich,[54] B. Kilminster,[40] D.H. Kim,[28] H.S. Kim,[28] J.E. Kim,[28] M.J. Kim,[12] S.B. Kim,[28]
S.H. Kim,[56] Y.K. Kim,[13] N. Kimura,[56] L. Kirsch,[6] S. Klimenko,[18] M. Klute,[33] B. Knuteson,[33] B.R. Ko,[16]
K. Kondo,[58] D.J. Kong,[28] J. Konigsberg,[18] A. Korytov,[18] A.V. Kotwal,[16] A. Kovalev,[46] A.C. Kraan,[46] J. Kraus,[24]
I. Kravchenko,[33] M. Kreps,[26] J. Kroll,[46] N. Krumnack,[4] M. Kruse,[16] V. Krutelyov,[10] T. Kubo,[56] S. E. Kuhlmann,[2]
T. Kuhr,[26] Y. Kusakabe,[58] S. Kwang,[13] A.T. Laasanen,[49] S. Lai,[34] S. Lami,[47] S. Lammel,[17] M. Lancaster,[31]
R.L. Lander,[7] K. Lannon,[40] A. Lath,[53] G. Latino,[47] I. Lazzizzera,[44] T. LeCompte,[2] J. Lee,[50] J. Lee,[28] Y.J. Lee,[28]
S.W. Lee[n],[54] R. Lefèvre,[3] N. Leonardo,[33] S. Leone,[47] S. Levy,[13] J.D. Lewis,[17] C. Lin,[61] C.S. Lin,[17] M. Lindgren,[17]
E. Lipeles,[9] T.M. Liss,[24] A. Lister,[7] D.O. Litvintsev,[17] T. Liu,[17] N.S. Lockyer,[46] A. Loginov,[61] M. Loreti,[44]
P. Loverre,[52] R.-S. Lu,[1] D. Lucchesi,[44] P. Lujan,[29] P. Lukens,[17] G. Lungu,[18] L. Lyons,[43] J. Lys,[29] R. Lysak,[14]
E. Lytken,[49] P. Mack,[26] D. MacQueen,[34] R. Madrak,[17] K. Maeshima,[17] K. Makhoul,[33] T. Maki,[23] P. Maksimovic,[25]
S. Malde,[43] G. Manca,[30] F. Margaroli,[5] R. Marginean,[17] C. Marino,[26] C.P. Marino,[24] A. Martin,[61] M. Martin,[21]
V. Martin[g],[21] M. Martínez,[3] T. Maruyama,[56] P. Mastrandrea,[52] T. Masubuchi,[56] H. Matsunaga,[56] M.E. Mattson,[59]
R. Mazini,[34] P. Mazzanti,[5] K.S. McFarland,[50] P. McIntyre,[54] R. McNulty[f],[30] A. Mehta,[30] P. Mehtala,[23]
S. Menzemer[h],[11] A. Menzione,[47] P. Merkel,[49] C. Mesropian,[51] A. Messina,[36] T. Miao,[17] N. Miladinovic,[6] J. Miles,[33]
R. Miller,[36] C. Mills,[10] M. Milnik,[26] A. Mitra,[1] G. Mitselmakher,[18] A. Miyamoto,[27] S. Moed,[20] N. Moggi,[5]

B. Mohr,[8] R. Moore,[17] M. Morello,[47] P. Movilla Fernandez,[29] J. Mülmenstädt,[29] A. Mukherjee,[17] Th. Muller,[26] R. Mumford,[25] P. Murat,[17] J. Nachtman,[17] A. Nagano,[56] J. Naganoma,[58] I. Nakano,[41] A. Napier,[57] V. Necula,[18] C. Neu,[46] M.S. Neubauer,[9] J. Nielsen,[29] T. Nigmanov,[48] L. Nodulman,[2] O. Norniella,[3] E. Nurse,[31] S.H. Oh,[16] Y.D. Oh,[28] I. Oksuzian,[18] T. Okusawa,[42] R. Oldeman,[30] R. Orava,[23] K. Osterberg,[23] C. Pagliarone,[47] E. Palencia,[11] V. Papadimitriou,[17] A.A. Paramonov,[13] B. Parks,[40] S. Pashapour,[34] J. Patrick,[17] G. Pauletta,[55] M. Paulini,[12] C. Paus,[33] D.E. Pellett,[7] A. Penzo,[55] T.J. Phillips,[16] G. Piacentino,[47] J. Piedra,[45] L. Pinera,[18] K. Pitts,[24] C. Plager,[8] L. Pondrom,[60] X. Portell,[3] O. Poukhov,[15] N. Pounder,[43] F. Prakoshyn,[15] A. Pronko,[17] J. Proudfoot,[2] F. Ptohos[e],[19] G. Punzi,[47] J. Pursley,[25] J. Rademacker[b],[43] A. Rahaman,[48] N. Ranjan,[49] S. Rappoccio,[22] B. Reisert,[17] V. Rekovic,[38] P. Renton,[43] M. Rescigno,[52] S. Richter,[26] F. Rimondi,[5] L. Ristori,[47] A. Robson,[21] T. Rodrigo,[11] E. Rogers,[24] S. Rolli,[57] R. Roser,[17] M. Rossi,[55] R. Rossin,[18] A. Ruiz,[11] J. Russ,[12] V. Rusu,[13] H. Saarikko,[23] S. Sabik,[34] A. Safonov,[54] W.K. Sakumoto,[50] G. Salamanna,[52] O. Saltó,[3] D. Saltzberg,[8] C. Sánchez,[3] L. Santi,[55] S. Sarkar,[52] L. Sartori,[47] K. Sato,[17] P. Savard,[34] A. Savoy-Navarro,[45] T. Scheidle,[26] P. Schlabach,[17] E.E. Schmidt,[17] M.P. Schmidt,[61] M. Schmitt,[39] T. Schwarz,[7] L. Scodellaro,[11] A.L. Scott,[10] A. Scribano,[47] F. Scuri,[47] A. Sedov,[49] S. Seidel,[38] Y. Seiya,[42] A. Semenov,[15] L. Sexton-Kennedy,[17] A. Sfyrla,[20] M.D. Shapiro,[29] T. Shears,[30] P.F. Shepard,[48] D. Sherman,[22] M. Shimojima[k],[56] M. Shochet,[13] Y. Shon,[60] I. Shreyber,[37] A. Sidoti,[47] P. Sinervo,[34] A. Sisakyan,[15] J. Sjolin,[43] A.J. Slaughter,[17] J. Slaunwhite,[40] K. Sliwa,[57] J.R. Smith,[7] F.D. Snider,[17] R. Snihur,[34] M. Soderberg,[35] A. Soha,[7] S. Somalwar,[53] V. Sorin,[36] J. Spalding,[17] F. Spinella,[47] T. Spreitzer,[34] P. Squillacioti,[47] M. Stanitzki,[61] A. Staveris-Polykalas,[47] R. St. Denis,[21] B. Stelzer,[8] O. Stelzer-Chilton,[43] D. Stentz,[39] J. Strologas,[38] D. Stuart,[10] J.S. Suh,[28] A. Sukhanov,[18] H. Sun,[57] T. Suzuki,[56] A. Taffard,[24] R. Takashima,[41] Y. Takeuchi,[56] K. Takikawa,[56] M. Tanaka,[2] R. Tanaka,[41] M. Tecchio,[35] P.K. Teng,[1] K. Terashi,[51] J. Thom[d],[17] A.S. Thompson,[21] E. Thomson,[46] P. Tipton,[61] V. Tiwari,[12] S. Tkaczyk,[17] D. Toback,[54] S. Tokar,[14] K. Tollefson,[36] T. Tomura,[56] D. Tonelli,[47] S. Torre,[19] D. Torretta,[17] S. Tourneur,[45] W. Trischuk,[34] R. Tsuchiya,[58] S. Tsuno,[41] N. Turini,[47] F. Ukegawa,[56] T. Unverhau,[21] S. Uozumi,[56] D. Usynin,[46] S. Vallecorsa,[20] N. van Remortel,[23] A. Varganov,[35] E. Vataga,[38] F. Vázquez[i],[18] G. Velev,[17] G. Veramendi,[24] V. Veszpremi,[49] R. Vidal,[17] I. Vila,[11] R. Vilar,[11] T. Vine,[31] I. Vollrath,[34] I. Volobouev[n],[29] G. Volpi,[47] F. Würthwein,[9] P. Wagner,[54] R.G. Wagner,[2] R.L. Wagner,[17] J. Wagner,[26] W. Wagner,[26] R. Wallny,[8] S.M. Wang,[1] A. Warburton,[34] S. Waschke,[21] D. Waters,[31] W.C. Wester III,[17] B. Whitehouse,[57] D. Whiteson,[46] A.B. Wicklund,[2] E. Wicklund,[17] G. Williams,[34] H.H. Williams,[46] P. Wilson,[17] B.L. Winer,[40] P. Wittich[d],[17] S. Wolbers,[17] C. Wolfe,[13] T. Wright,[35] X. Wu,[20] S.M. Wynne,[30] A. Yagil,[17] K. Yamamoto,[42] J. Yamaoka,[53] T. Yamashita,[41] C. Yang,[61] U.K. Yang[j],[13] Y.C. Yang,[28] W.M. Yao,[29] G.P. Yeh,[17] J. Yoh,[17] K. Yorita,[13] T. Yoshida,[42] G.B. Yu,[50] I. Yu,[28] S.S. Yu,[17] J.C. Yun,[17] L. Zanello,[52] A. Zanetti,[55] I. Zaw,[22] X. Zhang,[24] J. Zhou,[53] and S. Zucchelli[5]

(CDF Collaboration[*])

[1]Institute of Physics, Academia Sinica, Taipei, Taiwan 11529, Republic of China
[2]Argonne National Laboratory, Argonne, Illinois 60439
[3]Institut de Fisica d'Altes Energies, Universitat Autonoma de Barcelona, E-08193, Bellaterra (Barcelona), Spain
[4]Baylor University, Waco, Texas 76798
[5]Istituto Nazionale di Fisica Nucleare, University of Bologna, I-40127 Bologna, Italy
[6]Brandeis University, Waltham, Massachusetts 02254
[7]University of California, Davis, Davis, California 95616
[8]University of California, Los Angeles, Los Angeles, California 90024
[9]University of California, San Diego, La Jolla, California 92093
[10]University of California, Santa Barbara, Santa Barbara, California 93106
[11]Instituto de Fisica de Cantabria, CSIC-University of Cantabria, 39005 Santander, Spain
[12]Carnegie Mellon University, Pittsburgh, PA 15213
[13]Enrico Fermi Institute, University of Chicago, Chicago, Illinois 60637
[14]Comenius University, 842 48 Bratislava, Slovakia; Institute of Experimental Physics, 040 01 Kosice, Slovakia
[15]Joint Institute for Nuclear Research, RU-141980 Dubna, Russia
[16]Duke University, Durham, North Carolina 27708
[17]Fermi National Accelerator Laboratory, Batavia, Illinois 60510
[18]University of Florida, Gainesville, Florida 32611
[19]Laboratori Nazionali di Frascati, Istituto Nazionale di Fisica Nucleare, I-00044 Frascati, Italy
[20]University of Geneva, CH-1211 Geneva 4, Switzerland
[21]Glasgow University, Glasgow G12 8QQ, United Kingdom
[22]Harvard University, Cambridge, Massachusetts 02138
[23]Division of High Energy Physics, Department of Physics, University of Helsinki and Helsinki Institute of Physics, FIN-00014, Helsinki, Finland
[24]University of Illinois, Urbana, Illinois 61801

[25] *The Johns Hopkins University, Baltimore, Maryland 21218*
[26] *Institut für Experimentelle Kernphysik, Universität Karlsruhe, 76128 Karlsruhe, Germany*
[27] *High Energy Accelerator Research Organization (KEK), Tsukuba, Ibaraki 305, Japan*
[28] *Center for High Energy Physics: Kyungpook National University,*
Taegu 702-701, Korea; Seoul National University, Seoul 151-742,
Korea; and SungKyunKwan University, Suwon 440-746, Korea
[29] *Ernest Orlando Lawrence Berkeley National Laboratory, Berkeley, California 94720*
[30] *University of Liverpool, Liverpool L69 7ZE, United Kingdom*
[31] *University College London, London WC1E 6BT, United Kingdom*
[32] *Centro de Investigaciones Energeticas Medioambientales y Tecnologicas, E-28040 Madrid, Spain*
[33] *Massachusetts Institute of Technology, Cambridge, Massachusetts 02139*
[34] *Institute of Particle Physics: McGill University, Montréal,*
Canada H3A 2T8; and University of Toronto, Toronto, Canada M5S 1A7
[35] *University of Michigan, Ann Arbor, Michigan 48109*
[36] *Michigan State University, East Lansing, Michigan 48824*
[37] *Institution for Theoretical and Experimental Physics, ITEP, Moscow 117259, Russia*
[38] *University of New Mexico, Albuquerque, New Mexico 87131*
[39] *Northwestern University, Evanston, Illinois 60208*
[40] *The Ohio State University, Columbus, Ohio 43210*
[41] *Okayama University, Okayama 700-8530, Japan*
[42] *Osaka City University, Osaka 588, Japan*
[43] *University of Oxford, Oxford OX1 3RH, United Kingdom*
[44] *University of Padova, Istituto Nazionale di Fisica Nucleare,*
Sezione di Padova-Trento, I-35131 Padova, Italy
[45] *LPNHE, Universite Pierre et Marie Curie/IN2P3-CNRS, UMR7585, Paris, F-75252 France*
[46] *University of Pennsylvania, Philadelphia, Pennsylvania 19104*
[47] *Istituto Nazionale di Fisica Nucleare Pisa, Universities of Pisa,*
Siena and Scuola Normale Superiore, I-56127 Pisa, Italy
[48] *University of Pittsburgh, Pittsburgh, Pennsylvania 15260*
[49] *Purdue University, West Lafayette, Indiana 47907*
[50] *University of Rochester, Rochester, New York 14627*
[51] *The Rockefeller University, New York, New York 10021*
[52] *Istituto Nazionale di Fisica Nucleare, Sezione di Roma 1,*
University of Rome "La Sapienza," I-00185 Roma, Italy
[53] *Rutgers University, Piscataway, New Jersey 08855*
[54] *Texas A&M University, College Station, Texas 77843*
[55] *Istituto Nazionale di Fisica Nucleare, University of Trieste/ Udine, Italy*
[56] *University of Tsukuba, Tsukuba, Ibaraki 305, Japan*
[57] *Tufts University, Medford, Massachusetts 02155*
[58] *Waseda University, Tokyo 169, Japan*
[59] *Wayne State University, Detroit, Michigan 48201*
[60] *University of Wisconsin, Madison, Wisconsin 53706*
[61] *Yale University, New Haven, Connecticut 06520*
(Dated: December 5, 2006)

We present a measurement of the fractions F_0 and F_+ of longitudinally polarized and right-handed W bosons in top quark decays using data collected with the CDF II detector. The data set used in the analysis corresponds to an integrated luminosity of approximately 318 pb^{-1}. We select $t\bar{t}$ candidate events with one lepton, at least four jets, and missing transverse energy. Our helicity measurement uses the decay angle θ^*, which is defined as the angle between the momentum of the charged lepton in the W boson rest frame and the W momentum in the top quark rest frame. The $\cos\theta^*$ distribution in the data is determined by full kinematic reconstruction of the $t\bar{t}$ candidates. We find $F_0 = 0.85^{+0.15}_{-0.22}\,\text{(stat)} \pm 0.06\,\text{(syst)}$ and $F_+ = 0.05^{+0.11}_{-0.05}\,\text{(stat)} \pm 0.03\,\text{(syst)}$, which is consistent with the standard model prediction. We set an upper limit on the fraction of right-handed W bosons of $F_+ < 0.26$ at the 95% confidence level.

PACS numbers: 12.15.-y, 13.88.+e, 14.65.Ha, 14.70.Fm

*With visitors from [a]University of Athens, [b]University of Bristol, [c]University Libre de Bruxelles, [d]Cornell University,

[e]University of Cyprus, [f]University of Dublin, [g]University of Edinburgh, [h]University of Heidelberg, [i]Universidad Iberoameri-

I. INTRODUCTION

In 1995 the top quark was discovered at the Tevatron proton-antiproton collider at Fermilab by the CDF and DØ collaborations [1, 2]. It is the most massive known elementary particle and its mass is currently measured with a precision of about 1.3% [3, 4]. However, the measurements of other top quark properties are still statistically limited, so the question remains whether the standard model successfully predicts these properties. This paper addresses one interesting aspect of top quark decay, the helicity of the W boson produced in the decay $t \to W^+ b$.

At the Tevatron collider, with a center-of-mass energy $\sqrt{s} = 1.96$ TeV, most top quarks are pair-produced via the strong interaction. In the standard model the top quark decays predominantly into a W boson and a b quark, with a branching ratio close to 100%. The $V - A$ structure of the weak interaction of the standard model predicts that the W^+ bosons from the top quark decay $t \to W^+ b$ are dominantly either longitudinally polarized or left-handed, while right-handed W bosons are heavily suppressed and are forbidden in the limit of massless b quarks.

As a consequence of the Goldstone boson equivalence theorem [5, 6], the decay amplitude to longitudinal W bosons is proportional to the Yukawa coupling of the top quark; therefore, the decay rate scales with m_t^3, where m_t is the top quark mass. The longitudinal decay mode of the W boson is thereby linked to the spontaneous breaking of the electroweak gauge symmetry. The decay rate to transverse W bosons is governed by the gauge coupling and increases only linearly with m_t [7]. The fraction of longitudinally polarized W bosons is defined by

$$F_0 = \frac{\Gamma(t \to W_0^+ b)}{\Gamma(t \to W_{\rm L}^+ b) + \Gamma(t \to W_0^+ b) + \Gamma(t \to W_{\rm R}^+ b)} \; , \quad (1)$$

where W_0^+ stands for a longitudinally polarized W^+ boson, $W_{\rm L}^+$ for a left-handed W^+ boson, and $W_{\rm R}^+$ for a right-handed W^+ boson. The corresponding definitions for the W^- boson are implied. In leading-order perturbation theory F_0 is predicted to be $F_0 = \frac{m_t^2}{2m_W^2 + m_t^2}$ [8], where m_W is the mass of the W boson. Using $m_W = 80.43$ GeV/c^2 [9] and $m_t = (172.5 \pm 2.3)$ GeV/c^2 [3], gives $F_0 = 0.697 \pm 0.007$, where the given uncertainty is only due to the uncertainty in the top quark mass. Next-to-leading-order corrections to the total decay width and the partial decay width into longitudinal W bosons amount to about -10% [10–19]. However, the fraction of longitudinal W bosons is only negligibly changed.

cana, ^{j}University of Manchester, ^{k}Nagasaki Institute of Applied Science, ^{l}University de Oviedo, ^{m}University of London, Queen Mary and Westfield College, ^{n}Texas Tech University, ^{o}IFIC(CSIC-Universitat de Valencia),

A significant deviation from the predicted value for F_0 or a nonzero value for the right-handed fraction F_+ could indicate new physics. Left-right symmetric models [20], for example, lead to a significant right-handed fraction of W bosons in top quark decays. Such a right-handed component ($V + A$ coupling) would lead to a smaller left-handed fraction, while the longitudinal fraction F_0 would change insignificantly. Since the decay rate to longitudinal W bosons depends on the Yukawa coupling of the top quarks, the measurement of F_0 is sensitive to the mechanism of electroweak symmetry breaking. Alternative models for electroweak symmetry breaking, such as topcolor-assisted technicolor models, can lead to an altered F_0 fraction [21, 22].

The W boson polarization manifests itself in the decay $W \to \ell \nu$ in the angle θ^*, which is defined as the angle between the momentum of the charged lepton in the W rest frame and the W momentum in the top quark rest frame. For a longitudinal fraction F_0, a right-handed fraction F_+, and a left-handed fraction $F_- = 1 - F_+ - F_0$, the $\cos\theta^*$ distribution is given by [8]:

$$\begin{aligned}
\frac{dN}{d\cos\theta^*} &= (1 - F_+ - F_0) \cdot \frac{3}{8}(1 - \cos\theta^*)^2 \\
&+ (F_0) \cdot \frac{3}{4}(1 - \cos^2\theta^*) \\
&+ (F_+) \cdot \frac{3}{8}(1 + \cos\theta^*)^2. \quad (2)
\end{aligned}$$

In this analysis, the W helicity fractions are measured in a selected sample rich in $t\bar{t}$ events where one lepton, at least four jets, and missing transverse energy are required [23]. In order to calculate θ^*, all kinematic quantities describing the $t\bar{t}$ decays have to be determined.

Previous CDF measurements of the W helicity fractions in top quark decays used either the square of the invariant mass of the charged lepton and the b quark jet [24–26] or the lepton $p_{\rm T}$ distribution [25, 27] as a discriminant. The DØ collaboration used a matrix-element method to extract a value for F_0 [28]; in a second analysis the reconstructed distribution of $\cos\theta^*$ [29] was utilized to measure F_+. The previous measurement by CDF was $F_0 = 0.74^{+0.22}_{-0.34}$ [25], while DØ measured $F_0 = 0.56 \pm 0.31$ [28]. The CDF collaboration also measured the current best upper limit of $F_+ < 0.09$ at the 95% confidence level [26].

The organization of this paper is as follows. Section II describes the detector system relevant to this analysis. Section III illustrates the event selection of the $t\bar{t}$ candidates. The signal simulation and background estimation are given in Section IV. In Section V we describe our method to fully reconstruct $t\bar{t}$ pairs. The extraction of the helicity fractions is presented in Section VI. Section VII discusses the systematic uncertainties. Finally, the results and conclusions are given in Section VIII.

II. THE CDF II DETECTOR

A detailed description of the Collider Detector at Fermilab (CDF) can be found elsewhere [30]. A coordinate system with the z axis along the proton beam, azimuthal angle ϕ, and polar angle θ is used. The azimuthal angle is defined with respect to the outgoing radial direction and the polar angle is defined with respect to the proton beam direction. The transverse energy of a particle is defined as $E_T = E \sin \theta$. Throughout this paper we use pseudorapidity defined as $\eta = -\ln(\tan \frac{\theta}{2})$. The primary detector components relevant to this analysis are those which measure the energies and directions of jets, electrons, and muons and are briefly described below.

An open-cell drift chamber, the central outer tracker (COT) [31], and a silicon tracking system are used to measure the momenta of charged particles. The CDF II silicon tracker consists of three subdetectors: a layer of single-sided silicon microstrip detectors [32] glued on the beam pipe, a five layer double-sided silicon microstrip detector (SVX II) [33], and intermediate silicon layers [34] located at radii between 19 and 29 cm which provide linking between track segments in the COT and the SVX II. In the analysis presented in this article, the silicon tracker is used to identify jets originating from b quarks by reconstructing secondary vertices. The tracking detectors are located within a 1.4 T solenoid. Electromagnetic and hadronic sampling calorimeters [35–37], which have an angular coverage of $|\eta| < 3.6$, surround the tracking system and measure the energy flow of interacting particles. They are segmented into projective towers, each one covering a small range in pseudorapidity and azimuth. For electron identification the electromagnetic calorimeters are used, while jets are identified through the energy they deposit in the electromagnetic and hadronic calorimeter towers. The muon system [38] is located outside of the calorimeters and provides muon detection in the range $|\eta| < 1.5$. Muons penetrating the five absorption lengths of the calorimeters are detected in planes of multi-wire drift chambers. Since the collision rate exceeds the tape writing speed by five orders of magnitude, CDF has a three-level trigger system which reduces the event rate from 1.7 MHz to 60 Hz for permanent storage. The first two levels of trigger are implemented by special-purpose hardware, whereas the third one is implemented by software running on a computer farm.

III. SELECTION OF $t\bar{t}$ CANDIDATE EVENTS

In the decay channel considered in this analysis, one top quark decays semileptonically and the second top quark decays hadronically, leading to a signature of one charged lepton, missing transverse energy resulting from the undetected neutrino, and at least four jets. Candidate events are selected with high-p_T lepton triggers. The electron trigger requires a COT track matched to an energy cluster in the central electromagnetic calorime-

ter with $E_T > 18$ GeV. The muon trigger requires a COT track with $p_T > 18$ GeV/c matched to a track segment in the muon chambers. After offline reconstruction, we require exactly one isolated electron candidate with $E_T > 20$ GeV and $|\eta| < 1.1$ or exactly one isolated muon candidate with $p_T > 20$ GeV/c and $|\eta| < 1.0$. An electron or muon candidate is considered isolated if the E_T not assigned to the lepton in a cone of $R \equiv \sqrt{(\Delta\eta)^2 + (\Delta\phi)^2} = 0.4$ centered around the lepton is less than 10% of the lepton E_T or p_T, respectively. Jets are reconstructed by summing calorimeter energy in a cone of radius $R = 0.4$. The energy of the jets is corrected [39] for the η dependence of the calorimeter response, the time dependence of the calorimeter response, and the extra deposition of energy due to multiple interactions. Candidate jets must have corrected $E_T > 15$ GeV and detector $|\eta| < 2.0$. Detector η is defined as the pseudorapidity of the jet calculated with respect to the center of the detector. Events with at least four jets are accepted. At least one of the jets must be tagged as a b-jet by requiring a displaced secondary vertex within the jet [40]. The missing E_T ($\vec{\not{E}}_T$) is defined by

$$\vec{\not{E}}_T = -\sum_i E_T^i \hat{n}_i, \tag{3}$$

$$i = \text{calorimeter tower number with } |\eta| < 3.6,$$

where $\hat{n}_i$ is a unit vector perpendicular to the beam axis and pointing at the ith calorimeter tower. We also define $\not{E}_T = |\vec{\not{E}}_T|$. Because this calculation is based on calorimeter towers, $\not{E}_T$ has to be adjusted for the effect of the jet corrections for all jets with $E_T > 8$ GeV and detector $|\eta| < 2.5$. In events with muons, the transverse momentum of the muon is added to the sum, and a correction is applied to remove the average ionization energy released by the muon in traversing the calorimeter. We require the corrected $\not{E}_T$ to be greater than 20 GeV.

Additional requirements reduce the contamination from background. Electron events are rejected if the electron stems from a conversion of a photon. Cosmic ray muon events are also excluded. To remove Z boson events, we reject events in which the charged lepton can be paired with any more loosely defined jet or lepton to form an invariant mass consistent with the Z peak, defined as the range 76 GeV/c^2 to 106 GeV/c^2. After these selection requirements we find 82 $t\bar{t}$ candidates in the selected sample corresponding to an integrated luminosity of 318 pb^{-1}.

IV. SIGNAL SIMULATION AND BACKGROUND ESTIMATION

In order to determine the resolution of the kinematic quantities of the reconstructed $t\bar{t}$ pair, as well as to determine certain background rates, we utilize Monte Carlo simulations. The generated events are passed through

the CDF detector simulation [41] and are reconstructed in the same way as the measured data.

The simulated $t\bar{t}$ signal sample was generated with the PYTHIA generator [42] using a top quark mass of $m_t = 178$ GeV/c^2 which was the world average [43] of Run I. The values of F_0 and F_+ used in our standard model simulation are 0.7 and 0.0 respectively. To check the assumption that neither the efficiency nor the resolution due to the reconstruction depend on the values of F_0 and F_+, we use a customized version of the HERWIG Monte Carlo program [44] in which the helicity of one W boson is fixed to be longitudinal, left-handed, or right-handed.

The selected $t\bar{t}$ candidate sample contains a certain level of background contamination. Among the 82 observed events, we predict a background of 10.3 ± 1.9 events [23]. The dominant sources are W production in association with a quark-antiquark pair (31%), e.g. $\bar{q}q' \to Wgg$ with $g \to b\bar{b}$ ($c\bar{c}$) and $g \to q''\bar{q}''$, "mistagged" events (24%), in which a jet is erroneously tagged as a b-jet, and events where no W boson (non-W events) is produced (36%), e.g. direct $b\bar{b}$ production with additional gluon radiation. Additional sources are diboson (WW, WZ, ZZ) production (4.5%) and single-top production (4.5%). The non-W and mistag fractions are estimated using lepton trigger data. The W plus heavy flavor fraction is extracted using a sample of events simulated with ALPGEN [45]. The diboson and single-top rates are predicted based on their theoretical cross sections [46] and acceptances and efficiencies, which are derived from PYTHIA and MADEVENT [47] simulations.

V. FULL RECONSTRUCTION OF $t\bar{t}$ PAIRS

The measurement of $\cos\theta^*$ is based on fully reconstructing the top quarks through the four-momenta of the decay products. The challenge for the full reconstruction is to assign the observed jets to the decay products of the hadronically decaying W boson or the jets resulting from the b quarks from the top-quark decays. All possible assignments have to be considered. Thus, in each event there exist numerous hypotheses for the reconstruction of the $t\bar{t}$ pair. At the top quark reconstruction level, extra jet corrections are applied. The calorimeter energy is corrected to correspond to the energy of the traversing particle, the underlying event energy is subtracted, and, finally, the energy that is radiated outside the jet cone is added. The p_T vector of the neutrino is derived from $\vec{E}_T$. To calculate the z-component of the neutrino momentum, a quadratic constraint using the $W \to \ell\nu$ decay kinematics is used, with the assumption that the W boson mass equals the pole mass of 80.43 GeV/c^2. If the solution of the equation is complex, the real part of the solution is taken; otherwise the solution with the smaller value of $|p_{z,\nu}|$ is used. Adding the resulting four-momentum of the neutrino and the four-momentum of the charged lepton leads to the correct W boson four-vector in 78% of simulated events. In order to get all hypotheses for

the semileptonically decaying top quark, we consider all combinations of the four-momentum of one of the selected jets and the four-momentum of the W boson. The hadronically decaying W boson is then reconstructed by combining the four-momenta of two of the selected jets not assigned to the semileptonically decaying top quark. Adding the four-momenta of this W boson and of one of the remaining jets results in the hadronically decaying top quark. This procedure leads to $\frac{1}{2} \cdot N_{\text{jets}}!/(N_{\text{jets}} - 4)!$ different hypotheses for each event.

For simulated events it is possible to determine the hypothesis which is closest to the true event. This "best hypothesis" is defined as the hypothesis for which the deviation of the reconstructed top quarks and W bosons from the generated particles in the η-ϕ plane is minimal. Since this is not possible for measured data, we determine for each hypothesis a quantity Ψ which gives a quantitative estimate of how well this hypothesis matches the $t\bar{t}$ pair assumption, and we choose the hypothesis with the highest value of Ψ. Constraints on the mass of the hadronically decaying W boson, on the mass difference between both reconstructed top quark masses, on how b-like the jets assigned as b-jets in the $t \to Wb$ decays are, and on the reconstructed E_T of the two top quarks enter the computation of Ψ.

We define Ψ as

$$\Psi = \frac{1}{|\hat{f}_E - f_E| \cdot \chi^2} \cdot P_b \quad , \qquad (4)$$

where f_E is the sum of the transverse energies of the two top quarks divided by the total E_T of the event including $\not{E}_T$:

$$f_E = \frac{\sqrt{p_{T,t\to b\ell\nu}^2 + m_{t\to b\ell\nu}^2} + \sqrt{p_{T,t\to bjj}^2 + m_{t\to bjj}^2}}{\Sigma p_{T,\text{jet}} + \not{E}_T + E_{T,\ell}} \quad , \quad (5)$$

where $p_{T,t\to b\ell\nu}$ and $p_{T,t\to bjj}$ are the reconstructed transverse momenta of the semileptonically and hadronically decaying top quarks and $m_{t\to b\ell\nu}$ and $m_{t\to bjj}$ are the respective reconstructed top quark masses. The quantity $\Sigma p_{T,\text{jet}}$ is the sum of the transverse momenta of the four jets used in the $t\bar{t}$ event hypothesis. The transverse energy of the charged lepton is indicated with $E_{T,\ell}$. The motivation for the definition of f_E is that the E_T of the top quarks is approximately equal to the E_T of the entire event. The mean value $\hat{f}_E$ of the f_E distribution, obtained from the best hypothesis for each event of a $t\bar{t}$ Monte Carlo simulation, is determined to be 1.014.

The quantity χ^2 is defined as

$$\chi^2 = \frac{(m_{W\to jj} - \hat{m}_{W\to jj})^2}{\sigma_{m_{W\to jj}}^2} + \frac{(m_{t\to b\ell\nu} - m_{t\to bjj})^2}{\sigma_{\Delta m_t}^2} \quad , \quad (6)$$

where $m_{W\to jj}$ is the reconstructed mass of the hadronically decaying W boson and $m_{t\to b\ell\nu}$ and $m_{t\to bjj}$ are

TABLE I: Percentage of $t\bar{t}$ events that are reconstructed within a particular $\sum \Delta R$, as defined in Eq. 8.

	fraction [%]
best	30.2
$\sum \Delta R < 1.5$	41.5
$\sum \Delta R < 3.0$	57.9
$\sum \Delta R < 4.5$	66.4

the reconstructed mass of the semileptonically decaying top quark and the hadronically decaying top quark, respectively. The reconstructed mass of the hadronically decaying W boson should be equal to the mean value $\hat{m}_{W \to jj}$ within the resolution $\sigma_{m_{W \to jj}}$ and the difference between both top quark masses should be zero within the resolution $\sigma_{\Delta m_t}$. The values $\hat{m}_{W \to jj} = 79.5\,\mathrm{GeV}/c^2$, $\sigma_{m_{W \to jj}} = 10.2\,\mathrm{GeV}/c^2$, and $\sigma_{\Delta m_t} = 30.3\,\mathrm{GeV}/c^2$ that we use are obtained from the corresponding mass distributions using the best hypothesis of fully simulated $t\bar{t}$ events. The mass resolutions are dominated by the uncertainties in the jet energy reconstruction. The jet energy scale is determined from dijet data events and simulated samples and checked using γ+jet and Z+jet events [4, 48]. The value for $\hat{m}_{W \to jj}$ deviates from the measured W boson pole mass $m_W = 80.43\,\mathrm{GeV}/c^2$. The deviation is within the systematic uncertainties of the applied jet corrections.

The quantity P_b is a measure of how b-like the two jets assigned as such by the event reconstruction are, and is defined as:

$$P_b = (-\log \mathcal{P}_{t \to b\ell\nu} - \log \mathcal{P}_{t \to bjj}) \cdot 10^{N_{\mathrm{tag}}} , \quad (7)$$

where $\mathcal{P}_{t \to b\,\ell\nu}$ and $\mathcal{P}_{t \to b\,jj}$ are the probabilities that the jets chosen to be the b-jets from the semileptonically and hadronically decaying top quark are consistent with the hypothesis of a light quark jet with zero lifetime. This probability is calculated from the impact parameter of the tracks assigned to the jet in the r-ϕ plane [49]. The negative logarithm of that probability leads to large values for b-jets and small values for light flavor jets. However, since a reconstructed secondary vertex is a stronger indication for b-jets than the probability based on the impact parameter, the quantity P_b should be given a higher weight when there are secondary vertex tagged jets. Since $-\log \mathcal{P}$ nearly always takes values smaller than 10, the logarithmic sum is multiplied by the factor $10^{N_{\mathrm{tag}}}$, where N_{tag} is the number of b-tagged jets (either 0, 1 or 2).

In order to estimate the quality of the criterion for choosing the most probable event reconstruction based on the quantity Ψ, Monte Carlo studies are performed. We examine the sum of the distances in the η-ϕ plane associated with the semileptonically decaying top quark ($\Delta R_{t \to b\ell\nu}$), the hadronically decaying top quark ($\Delta R_{t \to bjj}$), and the hadronically decaying W boson ($\Delta R_{W \to jj}$).
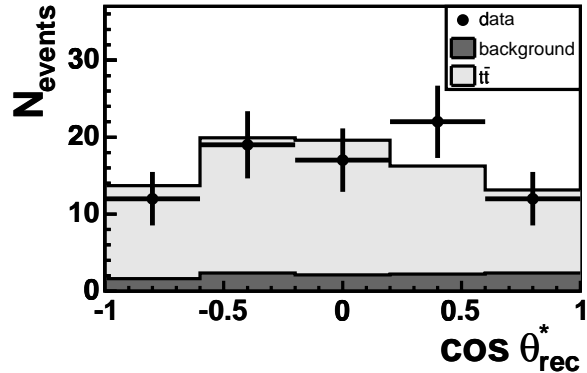

FIG. 1: Measured $\cos \theta^*_{\mathrm{rec}}$ distribution shown together with the estimated signal and background. The $t\bar{t}$ signal events are modeled by the standard model Monte Carlo generator PYTHIA with $m_t = 178\,\mathrm{GeV}/c^2$.

$$\sum \Delta R = \Delta R_{t \to b\ell\nu} + \Delta R_{t \to bjj} + \Delta R_{W \to jj}. \quad (8)$$

The distance ΔR between a generated ("gen") and a reconstructed ("rec") particle is given by $\Delta R = \sqrt{(\phi_{\mathrm{gen}} - \phi_{\mathrm{rec}})^2 + (\eta_{\mathrm{gen}} - \eta_{\mathrm{rec}})^2}$. Table I shows how often our selected hypothesis has a value of $\sum \Delta R$ below a given value. We also state the fraction of events in which the chosen hypothesis is the "best hypothesis" which is defined for each event as the hypothesis with the smallest value of $\sum \Delta R$.

Our reconstruction method yields $\cos \theta^*$ resolutions comparable to other methods used in previous CDF measurements [48]. In addition the present approach allows the inclusion of events with more than four jets in a consistent way.

Figure 1 shows the distribution of the measured $\cos \theta^*$ compared to the estimated signal and background distributions.

VI. EXTRACTION OF F_0 AND F_+ AND DETERMINATION OF THE DIFFERENTIAL $t\bar{t}$ PRODUCTION CROSS SECTION

Since the number of events in the data set is small, we do not simultaneously extract the fraction of longitudinally polarized and right-handed W bosons. We either fix F_+ to 0 and fit for F_0, or we fix F_0 to its expected value and fit for F_+. Thus, only one free parameter is used in each fit.

To extract the single free parameter (F_0 or F_+), we use a binned maximum likelihood method. The expected number of events in each bin is the sum of the expected background and signal. The latter is calculated from the theoretical $\cos \theta^*$ distributions (Eq. 2) for the three

helicities of the W boson. Integrating Eq. 2 for each bin i separately leads to a linear dependence of the expected number of signal events μ_i^{sig} on F_0 and F_+:

$$\mu_i^{\text{sig}} \propto (1 - F_0 - F_+) \cdot f_i^- + (F_0) \cdot f_i^0 + (F_+) \cdot f_i^+. \quad (9)$$

Here f^0, f^- and f^+ are defined as:

$$f_i^0 = \int_{a_i}^{b_i} \frac{3}{4}(1 - \cos^2\theta^*)d\cos\theta^*, \quad (10)$$

$$f_i^- = \int_{a_i}^{b_i} \frac{3}{8}(1 - \cos\theta^*)^2 d\cos\theta^*, \quad (11)$$

$$f_i^+ = \int_{a_i}^{b_i} \frac{3}{8}(1 + \cos\theta^*)^2 d\cos\theta^*, \quad (12)$$

where a_i (b_i) is the lower (upper) edge of the ith bin.

As mentioned above, the reconstruction of the $t\bar{t}$ process is not perfectly efficient. Thus, in order to calculate the number of signal events $\mu^{\text{sig,obs}}$ expected to be observed in a certain bin after the reconstruction, we consider acceptance and migration effects:

$$\mu_k^{\text{sig,obs}} \propto \sum_i \mu_i^{\text{sig}} \cdot \epsilon_i \cdot S(i,k). \quad (13)$$

The migration matrix element $S(i,k)$ gives the probability for an event which was generated in bin i to occur in bin k of the reconstructed $\cos\theta^*$ distribution. Since the acceptance depends on $\cos\theta^*$, we weight the contribution of each bin i with the efficiency ϵ_i. Both ϵ_i and $S(i,k)$ are determined using the standard model Monte Carlo generator PYTHIA, assuming that ϵ_i and $S(i,k)$ are independent of F_0 and F_+. This assumption has been verified using the customized HERWIG samples described above, which have fixed W helicities.

With the number of expected events and the number of observed events in each bin, we minimize the negative logarithm of the likelihood function by varying the free parameter F_0 or F_+.

In addition, an upper limit for F_+ at the 95% confidence level (CL) is computed by integrating the likelihood function $L(F_+)$. Since a Bayesian approach is pursued, we integrate only in the physical region $0 \leq F_+ \leq 0.3$ applying a prior distribution which is 1 in the interval [0,0.3] and 0 elsewhere.

In order to compare our observations with theory, the background estimate is subtracted from the selected sample. To correct for acceptance and reconstruction effects, a transfer function τ is calculated. The value τ_i for bin i is the ratio of the normalized number of theoretically expected events and the normalized number of events after applying all selection cuts and performing the reconstruction. For this calculation we use the fit result of F_0 or F_+. Multiplying the background-subtracted number of events in bin i with τ_i leads to the unfolded distribution. Subsequently, this distribution is normalized to the $t\bar{t}$ production cross section of $\sigma_{t\bar{t}} = 6.1 \pm 0.9$ pb [50, 51] assuming $m_t = 178$ GeV/c^2, which yields the desired distribution of the differential cross section.

VII. SYSTEMATIC UNCERTAINTIES

The systematic uncertainties caused by theoretical modeling, detector effects, and the analysis method have been studied using ensembles of simulated data samples. Each sample is made up of signal and background events drawn from the respective templates. The values for F_0 and F_+ are extracted using the same method as for the observed data sample. The systematic uncertainty for a certain source is then given by comparing the mean of the resulting F_0 and F_+ distributions of the corresponding ensemble with the default values.

We account for possible bias from Monte Carlo modeling of $t\bar{t}$ events by comparing HERWIG and PYTHIA event generators.

The contribution of the parton distribution function (PDF) uncertainty is determined by re-weighting the $t\bar{t}$ events generated with CTEQ5L [52] for different sets of PDFs. We add in quadrature the difference between MRST72 and MRST75 [53] and between the 20 pairs of CTEQ6M eigenvectors.

To estimate the influence of initial-state and final-state radiation, we use templates from PYTHIA Monte Carlo simulations in which the parameters for gluon radiation are varied to produce either less or more initial or final-state radiation [48] compared to the standard setup. The uncertainty due to the jet energy scale is quantified by varying the jet energy scale within its $\pm 1\sigma$ uncertainties [39]. We also investigate whether our method to choose one hypothesis for each single event contributes significantly to the total uncertainty. Since the probable influence due to the χ^2 and f_E terms in the computation of the quantity Ψ is already considered by varying the jet energy scale, we study the impact of P_b by omitting this term. To estimate the contribution of the background rate uncertainty, we simultaneously add or subtract, respectively, the values of one standard deviation of the estimated rates for the different processes. The uncertainty due to the background shape uncertainty is estimated by using each shape of the dominant three background distributions alone instead of using a composite of these shapes.

The uncertainties are listed in Table II. The largest contribution to the systematic uncertainty arises from the jet energy-scale uncertainty, followed by the uncertainty on the background shape.

Since the fraction of longitudinally polarized W bosons depends explicitly on the top quark mass, we do not include this dependence into the systematic uncertainties, but present our measurement assuming a certain top mass, namely 178 GeV/c^2.

However, we investigate the dependence of the measured F_0 and F_+ on the top quark mass. For a shift of $+5$ GeV/c^2 $(-5$ GeV/$c^2)$ in the top quark mass we estimate a deviation in F_0 of $+0.017 \pm 0.007$ (-0.017 ± 0.007), which corresponds within the errors to the theoretical prediction $F_0 = \frac{m_t^2}{2m_W^2 + m_t^2}$. The standard model predicts
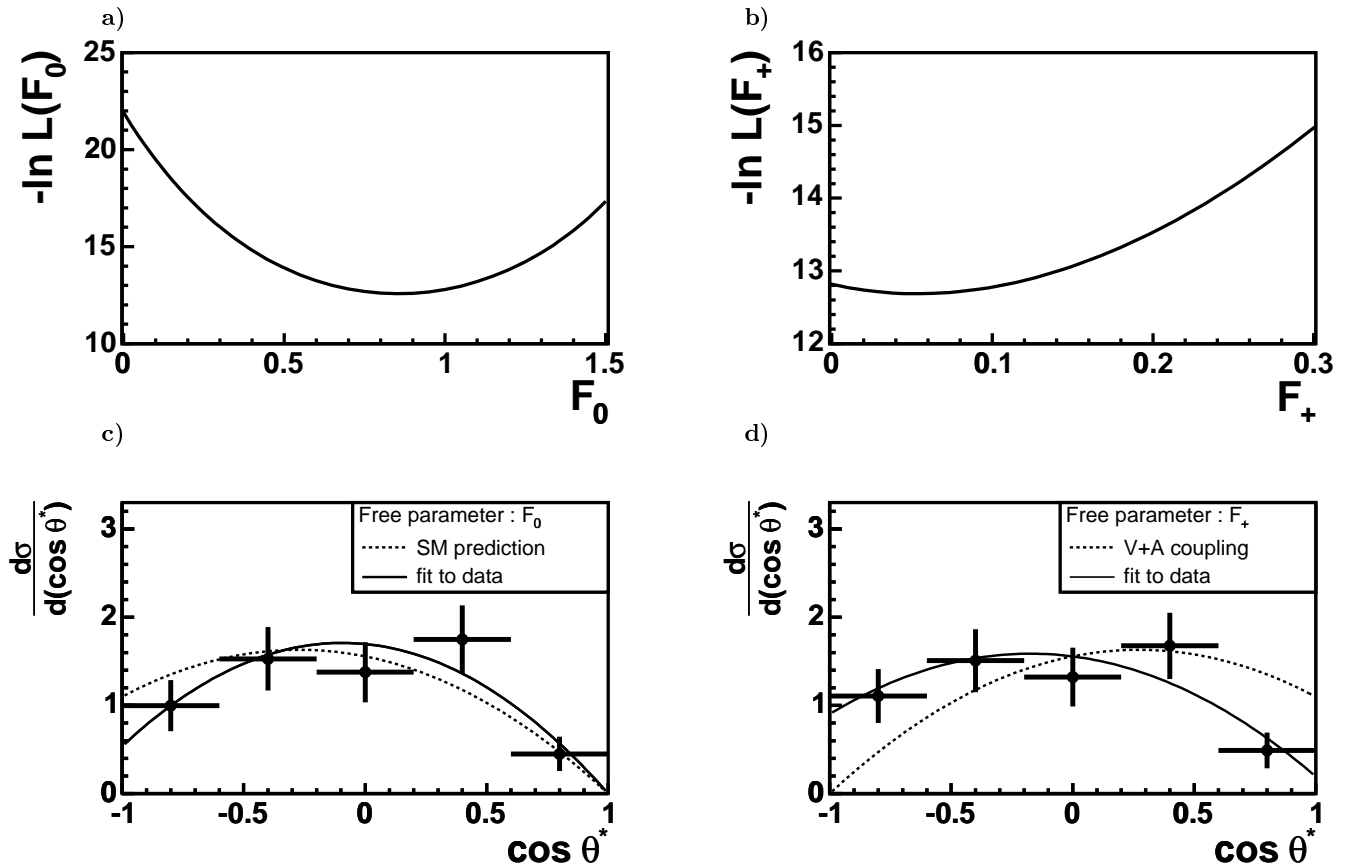
FIG. 2: Extraction of the longitudinal (F_0) and right-handed (F_+) fraction. For both fits F_0 and F_+ are used as single free parameter. In each case the other parameter is set to its expected standard model value. a,b) Negative log likelihood as a function of F_0 or F_+. c,d) Binned $\cos\theta^*$ distribution for data, corrected for acceptance and reconstruction effects. The distributions corresponding to the fit results $F_0 = 0.85$ and $F_+ = 0.05$ are shown as a continuous functions. The dashed curve shows the theoretical prediction for $F_0 = 0.7$ or for $F_+ = 0.3$.

TABLE II: Summary of systematic uncertainties. The total uncertainty is calculated by adding all the individual uncertainties in quadrature.

Source	$-\Delta F_0$	$+\Delta F_0$	$-\Delta F_+$	$+\Delta F_+$
Monte Carlo gen.	0.022	0.022	0.010	0.010
Parton distribution functions	0.017	0.017	0.006	0.006
Initial-state radiation	0.010	0.010	0.007	0.007
Final-state radiation	0.005	0.005	0.002	0.002
Jet energy scale	0.033	0.040	0.013	0.020
b-likeness of jet	0.009	0.009	0.008	0.008
Background normalization	0.002	0.004	0.000	0.003
Background shape	0.035	0.031	0.019	0.013
Total	**0.057**	**0.060**	**0.028**	**0.029**

see a small influence of the top quark mass on our measurement of F_+. For a shift of $+5$ GeV/c^2 (-5 GeV/c^2) in the top quark mass we estimate a deviation in F_+ of $+0.008 \pm 0.003$ (-0.008 ± 0.003).

VIII. RESULTS

We have presented a method for the measurement of the fractions F_0 and F_+ of longitudinally polarized and right-handed W bosons in top quark decays using a selected data sample with an integrated luminosity of approximately 318 pb^{-1} collected with the CDF II detector.

Taking the systematic uncertainties into account, assuming a top quark mass of $m_t = 178$ GeV/c^2, and assuming that the non-measured fraction is equal to the standard model expectation, the final result for the fractions of longitudinally polarized and right-handed W bosons is

$$F_0 = 0.85^{+0.15}_{-0.22}\,(\text{stat}) \pm 0.06\,(\text{syst}),$$

a top mass independent value for F_+ of zero, whereas we

$$F_+ = 0.05^{+0.11}_{-0.05} \text{ (stat) } \pm 0.03 \text{ (syst)}.$$

We obtain an upper limit on the fraction of right-handed W bosons of $F_+ \leq 0.26$ at the 95% CL. The systematic uncertainties are incorporated by convoluting $L(F_+)$ with a Gaussian with a mean of zero and a width equal to the total systematic uncertainty.

Figure 2a (b) shows the negative log-likelihood as a function of F_0 (F_+), where the minimum represents the result of the fit. Our method provides the possibility to correct the distribution of observed $\cos\theta^*$ for the selected sample for acceptance and reconstruction effects. Figures 2c and 2d show the unfolded distribution, normalized to the theoretical $t\bar{t}$ cross section, in comparison with theoretical predictions for standard model and a $V + A$ model in the case of F_+. As one can see, the observation is compatible with the standard model prediction. Also the measured values for F_0 and F_+ are in good agreement with the standard model.

IX. ACKNOWLEDGMENTS

[1] F. Abe et al. (CDF Collaboration), Phys. Rev. Lett. **74**, 2626 (1995).

[2] S. Abachi et al. (DØ Collaboration), Phys. Rev. Lett. **74**, 2632 (1995).

[3] T. E. W. Group (Tevatron Electroweak Working Group) (2006), hep-ex/0603039.

[4] A. Abulencia et al. (CDF Collaboration), Phys. Rev. Lett. **96**, 022004 (2006).

[5] J. M. Cornwall, D. N. Levin, and G. Tiktopoulos, Phys. Rev. D **10**, 1145 (1974).

[6] B. W. Lee, C. Quigg, and H. B. Thacker, Phys. Rev. D **16**, 1519 (1977).

[7] J. H. Kühn (1996), Lectures delivered at 23rd SLAC Summer Institute, hep-ph/9707321.

[8] G. L. Kane, G. A. Ladinsky, and C. P. Yuan, Phys. Rev. D **45**, 124 (1992).

[9] S. Eidelman et al. (Particle Data Group), Phys. Lett. B **592** (2004).

[10] M. Jezabek and J. H. Kühn, Nucl. Phys. **B 314**, 1 (1989).

[11] M. Jezabek and J. H. Kühn, Phys. Lett. B **207**, 91 (1988).

[12] A. Czarnecki and K. Melnikow, Nucl. Phys. **B 544**, 520 (1999).

[13] K. G. Chetyrkin, R. Harlander, T. Seidensticker, and M. Steinhauser, Phys. Rev. D **60**, 114015 (1999).

[14] A. Denner and T. Sack, Nucl. Phys. **B 358**, 46 (1991).

[15] R. Migneron, G. Eilam, R. R. Mendel, and A. Soni, Phys. Rev. Lett. **66**, 3105 (1991).

[16] M. Fischer, S. Groote, J. G. Korner, M. C. Mauser, and B. Lampe, Phys. Lett. B **451**, 406 (1999).

[17] M. Fischer, S. Groote, J. G. Korner, and M. C. Mauser, Phys. Rev. D **63**, 031501 (2001).

[18] M. Fischer, S. Groote, J. G. Korner, and M. C. Mauser, Phys. Rev. D **65**, 054036 (2002).

[19] H. S. Do, S. Groote, J. G. Korner, and M. C. Mauser, Phys. Rev. D **67**, 091501 (2003).

[20] R. D. Peccei, S. Peris, and X. Zhang, Nucl. Phys. **B 349**, 305 (1991).

[21] X.-L. Wang, Q.-L. Zhang, and Q.-P. Qiao, Phys. Rev. D **71**, 014035 (2005).

[22] C.-R. Chen, F. Larios, and C. P. Yuan, Phys. Lett. B **631**, 126 (2005).

[23] A. Abulencia et al. (CDF Collaboration), Phys. Rev. Lett. **97**, 082004 (2006).

[24] D. Acosta et al. (CDF Collaboration), Phys. Rev. D **71**, 031101 (2005).

[25] A. Abulencia et al. (CDF Collaboration), Phys. Rev. D **73**, 111103 (2006).

[26] A. Abulencia (2006), submitted to Phys. Rev. Lett., hep-ex/0608062.

[27] A. Affolder et al. (CDF Collaboration), Phys. Rev. Lett. **84**, 216 (2000).

[28] V. M. Abazov et al. (DØ Collaboration), Phys. Lett. B **617**, 1 (2005).

[29] V. M. Abazov et al. (DØ Collaboration), Phys. Rev. D **72**, 011104 (2005).

[30] D. Acosta et al. (CDF Collaboration), Phys. Rev. D **71**, 032001 (2005).

[31] A. Affolder et al. (CDF Collaboration), Nucl. Instrum. Methods A **526**, 249 (2004).

[32] C. S. Hill (CDF Collaboration), Nucl. Instrum. Methods A **530**, 1 (2004).

[33] A. Sill (CDF Collaboration), Nucl. Instrum. Methods A **447**, 1 (2000).

[34] A. Affolder et al. (CDF Collaboration), Nucl. Instrum.

Methods A **453**, 84 (2000).

[35] L. Balka *et al.* (CDF Collaboration), Nucl. Instrum. Methods A **267**, 272 (1988).

[36] S. Bertolucci *et al.* (CDF Collaboration), Nucl. Instrum. Methods A **267**, 301 (1988).

[37] M. G. Albrow *et al.* (CDF Collaboration), Nucl. Instrum. Methods A **480**, 524 (2002).

[38] G. Ascoli *et al.*, Nucl. Instrum. Methods A **268**, 33 (1988).

[39] A. Bhatti *et al.*, Nucl. Instrum. Methods A **566**, 375 (2006).

[40] D. Acosta *et al.* (CDF Collaboration), Phys. Rev. D **71**, 052003 (2005).

[41] E. Gerchtein and M. Paulini (2003), Talk given at 2003 Conference on Computing in High-Energy and Nuclear Physics, physics/0306031.

[42] T. Sjostrand *et al.*, Comput. Phys. Commun. **135**, 238 (2001).

[43] P. Azzi *et al.* (CDF Collaboration) (2004), hep-ex/0404010.

[44] G. Corcella *et al.*, J. High Energy Phys. **01**, 010 (2001).

[45] M. L. Mangano, M. Moretti, F. Piccinini, R. Pittau, and A. D. Polosa, J. High Energy Phys. **07**, 001 (2003).

[46] J. M. Campbell and R. K. Ellis, Phys. Rev. D **60**, 113006 (1999).

[47] F. Maltoni and T. Stelzer, J. High Energy Phys. **02**, 027 (2003).

[48] A. Abulencia *et al.* (CDF Collaboration), Phys. Rev. D **73**, 032003 (2006).

[49] A. Abulencia *et al.* (CDF Collaboration) (2006), hep-ex/0607035.

[50] M. Cacciari, S. Frixione, M. L. Mangano, P. Nason, and G. Ridolfi, J. High Energy Phys. **04**, 068 (2004).

[51] N. Kidonakis and R. Vogt, Phys. Rev. D **68**, 114014 (2003).

[52] H. L. Lai *et al.* (CTEQ Collaboration), Eur. Phys. J. C **12**, 375 (2000).

[53] A. D. Martin, R. G. Roberts, W. J. Stirling, and R. S. Thorne, Eur. Phys. J. C **4**, 463 (1998).